行政院國家科學委員會專題研究計畫成果報告

廣義的機會式通訊：無線行動網路中之競爭、合作與感知－

子計畫一:感知無線行動網路之頻譜偵測與管理

Generalized Opportunistic Communications: Competition, Cooperation and Cognition in Wireless Mobile Networks:
Spectrum sensing and management in cognitive wireless mobile networks

計畫編號：NSC 96-2221-E-009-076-MY3

執行期間： 96/08/01~97/07/31

主持人：蘇育德教授　國立交通大學電信工程學系

計畫參與人員：劉人仰、蘇郁文、謝易霖

中文摘要

感知無線通訊系統需要準確的頻譜感測能力。在本報告中，我們分析一種名叫轉換域通訊系統(TDCS)的感知展頻無線通訊技術對頻譜感測誤差的敏感度。頻率轉換通訊系統是一個多載波的感知展頻系統。它所使用複數展頻序列之多載波皆須位於傳送端或（和）接收端所偵測出的空白頻帶。我們分析當其中一端或是兩端的頻譜估測有錯誤（兩端頻譜的估測是獨立的）時造成頻譜不匹配的影響。我們分析了頻譜匹配誤差造成的系統錯誤率增高。估測錯誤機率降低或子載波數目增加都可改善系統效能及強健度。此外，相較於傳送端，接收端頻譜估測誤差對於系統效能影響較大。

關鍵詞: 感知無線通訊，頻率轉換通訊系統，頻譜估測。

Abstract

We analyze the effect of spectral mismatches on the performance of a cognitive spread spectrum (SS) system called the transform domain communication system (TDCS), which uses a multicarrier based complex spreading sequence. As the locations of the carriers are estimated spectrum holes, the system performance depends heavily on the spectrum sensing accuracy.

This report analyzes the effect of discrete spectrum estimation errors on one or both sides of such a TDCS link. The discrete spectrum estimation is carried out in a per-channel detection manner, i.e., both sides independently determine which subcarriers (channels) within the SS band are available. Our analysis indicates that an irreducible error floor arises due to spectrum estimation errors. As expected, the bit error probability performance improves and the error floor is reduced when the probability of single subcarrier detection error p decreases and/or the number of subcarriers increases. We also find that the system performance is more sensitive to the receiver's than to the transmitter's spectrum estimation error.

Keywords: cognitive radio, TDCS, spectrum sensing

1. Introduction

Current spectrum management policy follows a fixed band (channel) assignment scheme which results in inefficient spectrum usage. It was observed [2] that on the average only two percent of the allocated spectrum is actually in use at any given moment and location. Cognitive radio (CR) which allows distributed dynamic spectrum usage was therefore proposed to remedy such a shortcoming in spectrum management. Based on the CR concept, Chakravarthy *et al.* [2] proposed a dynamic modified direct-sequence spread spectrum (DS-SS) system to which they referred as adaptive waveform communication system (AWCS). Since the spreading sequence of AWCS is synthesized in the transform domain, the system is also called transform domain communication system (TDCS).

The basic idea behind TDCS is to generate a spreading sequence whose spectrum avoids existing users or jammers within the SS band. The spectrum conditions at transmitter and receiver are independently estimated at both sides. If the spectrum seen (or measured) by transmitter is different from that seen at receiver, the mismatch between two spreading sequence spectra will cause performance degradation [3]. Spectra mismatches arise because of geographic separation and/or spectrum estimation errors, i.e., either the ``true" spectrum represented at two sides are different or the estimated spectra are different although the spectrum representation are the same. In this report, we analyze the effect of spectrum estimation error induced spectrum mismatches on the symbol error rate (SER) performance in additive white Gaussian noise (AWGN) and Rayleigh fading channels, respectively.

The rest of this report is organized as followed. Section II gives an overview of the TDCS technique. The detailed description can be found in [1]. Performance analysis of BPSK-TDCS in AWGN channels and related simulation results are presented in Section III. We then extend our investigation to the case of arbitrary amplitude/phase modulation in AWGN and Rayleigh fading channels. The last section provides conclusion and suggest some future research works.

II. An introduction to TDCS

The basic idea behind TDCS is to produce a so-called time-domain fundamental modulation waveform (FMW) or a complex spreading sequence which avoids existing users or jammers by dynamically selecting the subcarriers used over a given bandwidth. A block diagram of the TDCS transmitter is illustrated in Fig. 1. The transmitter partitions the signal band into N equal-spaced subbands (tones) and performs spectrum estimation to determine which subbands are being used. The spectrum estimator output is an N-dimensional binary vector $\mathbf{A_x} = (A_x(w_0), A_x(w_1), \ldots, A_x(w_{N-1}))$ with $A_x(w_i) = 1$ or 0 depending on whether the i-th subband is available (1) or not (0). The subscript x will be Tx or Rc to denote if the vector is associated with the transmitter (Tx) or the receiver (Rc). The binary vector $\mathbf{A_{Tx}}$ is multiplied element-wise by a user-specific random vector e^{jw_i} and scaled by constant factor before being inverse discrete Fourier transformed to produce the time-domain FMW. The multiplication of the random vector is to make the FMW noise-like and to provide the multiple access capability. The FMW is used to spread (or as a carrier of) the binary phase shift keying (BPSK) or cyclic code shift keying (CCSK) modulated data sequence.

Although TDCS seems to be similar to an OFDM or a muticarrier OFDM system, there are several distinctions between the them. For example, in an OFDM system the number of subcarriers (subbands) is fixed while the number of subbands used in TDCS is dependent on the need or the environment. A detailed comparison can be found in [1]. When the only channel impairment is AWGN, a BPSK-modulated TDCS system with perfect spectrum estimation and matches on both sides of the link yields bit error probability P_e given by

$$P_e = Q\left(\sqrt{\frac{2E_b}{N_0}}\right), \quad (1)$$

where $Q\left(\sqrt{x}\right) \equiv \frac{1}{\sqrt{2\pi}} \int_x^{\infty} e^{-\frac{y^2}{2}} dy$.

III. Performance Analysis of BPSK-TDCS in AWGN

As defined in Section II, $\mathbf{A}_{\mathbf{Tx}}$, $\mathbf{A}_{\mathbf{Rc}}$ are the binary-valued random variables that represent the transmitter's and the receiver's spectrum estimators outputs. $\mathbf{A}_{\mathbf{tx}}(w)$ =1 means the transmitter believes w is available while $\mathbf{A}_{\mathbf{tx}}(w)=0$ implies otherwise. Similar interpretation is attached to $\mathbf{A}_{\mathbf{Rc}}$.

Depending on the geographic distribution of wireless network users, the true spectra seen from both sides can be identical or different and spectrum mismatches might still arise even if the spectral estimations at both sides are error-free. We refer to such spectra mismatches as network geography induced spectra mismatches.

Mismatches are most likely to occur when the distance between two sides of the link is large. To simplify our analysis we define the true spectrum as such that no existing user is interfered by the transmitted signal and the received waveform is not interfered by any existing user if error-free spectrum estimates are available on both sides of the link. The true spectrum represented by the binary-valued ***N***-dimensional vector $\mathbf{A}=(A(w_0),A(w_1),\ldots,A(w_{N-1}))$, where ***N*** is the size of inverse discrete fourier transform (IDFT), is thus related to the error-free spectrum estimates $\mathbf{A}_{Tx}^0$ and $\mathbf{A}_{Rc}^0$ via $\mathbf{A}=\mathbf{A}_{Tx}^0 \wedge \mathbf{A}_{Rc}^0$, where $\wedge$ denotes component-wise logical "and" operation.

Example: Network geography induced spectra mismatch

Suppose the spectral estimations at both sides of a 4-channel (***N*** = 4) link are error-free and $\boldsymbol{A}_{Tx}$ = (0,1,1,0) and $\boldsymbol{A}_{Rc}$ = (0,1,1,0). The mismatch arises from the fact that the transmitter-centered geographic locations and distances of the existing spectrum users are different from the receiver-centered ones. There is a primary user using the first channel whose location is very close to the transmitter but is far away from the receiver. On the other hand, someone near the receiver is using channel two but it is far away from the transmitter. For this case, the true spectrum is given by ***A*** = (0,0,1,0).

We shall assume that $A(w_i)=0$ with probability 1 - P_{sa} and $A(w_i)=1$ with probability P_{sa}. Define two complementary sets of subbands (channels)

$$\mathbf{G}_0 = \{w_i \mid A(w_i)=0, 0 \le i \le N-1\}$$
$$\mathbf{G}_1 = \{w_i \mid A(w_i)=1, 0 \le i \le N-1\}.$$

$\mathbf{G}_0$ contains all subbands that are currently in use and $\mathbf{G}_1$ is the set of available (unused) subbands. Let $|\mathbf{G}_1| = N_1$ be the cardinality of $\mathbf{G}_1$, then $|\mathbf{G}_0| = N - N_1$.

Obviously, eight possible scenarios may

occur, as listed in Table 1. For Cases 1, and 3, interference from existing users is present. In Cases 1 and 5, (additional) noise within the subband w will be received. The received signal energy is reduced in Cases 2 and 6. If the spectrum estimation is performed in a per-channel manner and each channel is independently used, then it is reasonable to assume that the following four probabilities,

$P_{t0} = \Pr(A_{Tx}(w) = 1 \mid A(w) = 1)$

$P_{t1} = \Pr(A_{Tx}(w) = 0 \mid A(w) = 0)$

$P_{r0} = \Pr(A_{Rc}(w) = 1 \mid A(w) = 1)$

$P_{t0} = \Pr(A_{Rc}(w) = 0 \mid A(w) = 0)$

and their complementary probabilities are independent of w_i. These assumptions imply that $\mathbf{A}$is binomial distributed with parameter P_{sa} and furthermore, $\mathbf{A}_{\mathbf{Tx}}$ and $\mathbf{A}_{\mathbf{Rc}}$ are obtained by modifying $\mathbf{A}$ based on P_{t0}, P_{r0}, P_{t1}, and P_{r1}, respectively.

To begin with, we consider the case P_{sa} = 0.5. It can be proved that in a AWGN channel with one-sided power spectral density of N_0 W/Hz, the bit error rate (BER) expression is given by (2) shown in the last page of this report where we assume that each (independent) incorrectly estimated subband cause additional interference that is represented by a zero-mean Gaussian random variable with identical variance $N_I/2$. Furthermore, the error floor is given by

$$P_{ef} = \left(\frac{1}{2}\right)^{N+1} (1 - P_{t0}P_{r0} + P_{t1} + P_{r1} - P_{t1}P_{r1})^N \quad (3)$$

A. Perfect spectral estimation at the transmitter side

If $P_{t0} = P_{t1} = 1$, i.e., the transmitter's spectral estimation is perfect, then the bit error rate becomes

$$P_b = \sum_{N_1=0}^{N} \sum_{i=0}^{N_1} \sum_{j=0}^{N-N_1} \binom{N}{N_1} \left(\frac{1}{2}\right)^N \binom{N_1}{i} P_{r0}^i (1-P_{r0})^{N_1-i} \binom{N-N_1}{j} P_{r1}^{N-N_1-j} (1-P_{r1})^j \, Q\left(\sqrt{\frac{2E_b(\frac{i}{N_1})}{N_0\left(1+\frac{j}{\max(i,1)}\right) + \frac{j}{\max(i,1)} N_I}}\right) \quad (4)$$

When $E_b \to \infty$, every terms on the right hand side of the above equation except for the term corresponding to i = 0 approach zero and the corresponding error floor becomes

$$P_{ef} = \frac{1}{2}\left(1 - \frac{P_{r0}}{2}\right)^N \quad (5)$$

This implies that the error floor depends on P_{r0} and ***N*** only.

Note that if the case N_1 =0, i.e., the transmitter knows that no subband is available but the receiver does not, can somehow be avoided, e.g., the transmitter sends a special tone to the receiver whenever it detects the ``no vacancy'' condition, then the error floor becomes

$$\frac{1}{2}\left(\left(1 - \frac{P_{r0}}{2}\right)^N - \frac{1}{2^N}\right) \quad (6)$$

B. Perfect spectral estimation at the receiver side

When $P_{r0} = P_{r1} = 1$ the BER is given by

$$P_b = \sum_{N_1=0}^{N} \sum_{i=0}^{N_1} \sum_{j=0}^{N-N_1} \binom{N}{N_1} \left(\frac{1}{2}\right)^N \binom{N_1}{i} P_{t0}^i (1-P_{t0})^{N1-i} \binom{N-N_1}{j} P_{t1}^{N-N_1-j} (1-P_{t1})^j \, Q\left(\sqrt{\frac{2E_b(\frac{i}{\max(i+j,1)})}{N_0\left(1+\frac{N_1-i}{\max(i,1)}\right)}}\right) \quad (7)$$

The error floor expression can be obtained by substituting P_{r0} by P_{t0} in (5). Similarly, when N_1 =0, the receiver should notify the transmitter to stop sending signal. If this is feasible the error floor is obtained by replacing P_{r0} with P_{t0} in (6).

C. Spectral estimation match at both sides

In case the transmitter and receiver can somehow exchange their spectral estimates then

$$P_b = \sum_{N_1=0}^{N}\sum_{i=0}^{N_1}\sum_{j=0}^{N-N_1}\sum_{k_1=0}^{i}\sum_{l_1=0_{k_1+l_1\neq 0}}^{j} \binom{N}{N_1}\frac{1}{C_m}\left(\frac{1}{2}\right)^N \binom{N_1}{i}P_{t0}^i(1-P_{t0})^{N1-i}\binom{N-N_1}{j}P_{t1}^{N-N_1-j}(1-P_{t1})^j \binom{i}{k_1}P_{r0}^{k_1}(1-P_{r0})^{i-k_1}\binom{j}{l_1}P_{r1}^{j-l_1}(1-P_{r1})^{l_1} Q\left(\sqrt{\frac{2E_b}{N_o+\frac{l_1}{\max(k_1+l_1,1)}N_I}}\right) \quad (8)$$

where

$$C_m = 1-\left(\frac{1}{2}\right)^N(1-P_{r0}P_{t0}+P_{t1}+(1-P_{t1})P_{r1})^N$$

D. Discussion

The BER performance difference between Case A (N_1 could be zero) and Case B ($N_1 \neq 0$) if one side of the link has perfect spectrum hole information is $(0.5)^{N+1}$, which is small when N is large. That is, both cases yield similar bit error rate if N is large.

To investigate the sensitivities of spectral estimation error at both sides, we compare (4) and (7) and assume that $P_0 = P_{t0} = P_{r0}$ and $P_0 = P_{t0} = P_{r0}$.

$$P_\Delta = \sum_{N_1=0}^{N}\sum_{i=0}^{N_1}\sum_{j=0}^{N-N_1}\binom{N}{N_1}\left(\frac{1}{2}\right)^N\binom{N_1}{i} P_0^i(1-P_0)^{N_1-i}\binom{N-N_1}{l_2}P_1^{N-N_1-j}(1-P_1)^j f_e \quad (9)$$

where

$$f_e = Q\left(\sqrt{\frac{2E_b\left(\frac{i}{\max(i+j,1)}\right)}{N_0\left(1+\frac{N_1-i}{\max(i,1)}\right)}}\right) - Q\left(\sqrt{\frac{2E_b\left(\frac{i}{N_1}\right)}{N_0\left(1+\frac{j}{\max(i,1)}\right)+\frac{j}{\max(i,1)}N_I}}\right) \leq 0 \quad (10)$$

This result has been expected due to the existence of interference and it can be proved that $f_e = 0$ when there is no interference. Hence, the spectral estimation at receive side is more important than that at transmit side

E. Simulation results

In this section, we show that the simulation of the performance of TDCS agrees with (2) for different cases. The size of IDFT N is set equal to 8.

Example 2: The effect of P_{t0}.

The effect of P_{t0} is illustrated in Fig. 2. The parameters are set as followed: P_{t1} =0.5, P_{r0} =0.7, P_{r1} =0.4 and $\frac{E_b}{N_I}$ =0 dB. It is obvious that the simulation result is almost identical to what has been predicted by analysis.

Example 3: The effect of P_{r0} and P_{r1}.

Fig. 3 plots the simulated performance with varying P_{r0} and P_{r1}. Again, our analytic result is validated by computer simulation. The other parameter values used are: P_{t0} =0.9, P_{t1}=0.5 and $\frac{E_b}{N_I}$ =0 dB. Notice that the values of P_{r0} and P_{r1} imply

$$A_{Rc}(w) = \begin{cases} 1, & \text{with } P_{r0} \\ 0, & \text{with } P_{r1} = 1-P_{r0} \end{cases},$$

i.e., it is determined by receiver without considering the environment. It is a good strategy to always assign $A(w) = 1$ without estimating the spectrum at the receive side.

Example 4: The effect of P_{t1}

The effect of P_{t1} is plotted in Fig. 4. We can see that they are almost identical. The parameter values used are: $P_{t0} = P_{r0} = P_{r1}$ =0.9 and $\frac{E_b}{N_I}$ =0 dB. An interesting observation is that the BER curves have different cross-over points for different P_{t1}. This is due to the fact that only $j = N - N_1$ has nonzero value in (2) if P_{t1}=0. Since $j = N - N_1$, $l_2 = 0$. This implies it is possible that the interference is smaller than that in other cases at high $\frac{E_b}{N_0}$. To illustrate this argument, consider Fig. 5. where it is assumed that $P_{t0} = P_{r0} = 1$, and $\frac{E_b}{N_I}$=0 dB. When P_{r1} =0.7, the interference is more serious and centered at higher l_1 than that in P_{r1}=0.9. For P_{t1}=0, it is possible to reduce interference at cost of E_b, which can be expected by noticing

$$P_b = \sum_{N_1=0}^{N} \sum_{l_1=0}^{N-N_1} \binom{N}{N_1} \frac{1}{2}^N \binom{N-N_1}{l_1} P_{r1}^{N-N_1-l_1} (1-P_{r1})^{l_1} f \quad (11)$$

where

$$f = \begin{cases} Q\left(\sqrt{\dfrac{2E_b\left(\frac{N_1+l_1}{\max(N,1)}\right)}{\frac{l_1}{\max(N_1+l_1,1)}N_I}}\right), & P_{t1}=0 \\ Q\left(\sqrt{\dfrac{2E_b\left(\frac{N_1}{\max(N_1,1)}\right)}{\frac{l_1}{\max(N_1,1)}N_I}}\right), & P_{t1}=1 \end{cases}$$

V. Amplitude/Phase modulations in AWGN and Rayleigh channels

With the same notation in Section III, the SER in AWGN for coherent demodulation is given by (12) shown in the last page, where P_e is summarized in Table II.

TABLE II
P_e IN AWGN

$P_e(x)$	Modulation Type
$Q(2\sqrt{x})$	BPSK
$1-[1-Q(\sqrt{x})]^2$	QPSK
$\frac{1}{\pi}\int_0^{\frac{(M-1)\pi}{M}} \exp\left[\frac{-\sin^2(\pi/M)x}{\sin^2\phi}\right]d\phi$	MPSK
$\frac{2(M-1)}{M}Q\left(\sqrt{\frac{6x}{M^2-1}}\right)$	MPAM
$1-\left(1-\frac{2(\sqrt{M}-1)}{\sqrt{M}}Q\left(\sqrt{\frac{3x}{M-1}}\right)\right)^2$	MQAM

The error floor becomes

$$P_s = C\left[P_{sa}(1-P_{t0}P_{r0}) + (1-P_{sa})(P_{t1}+P_{r1}-P_{t1}P_{r1})\right]^N \quad (13)$$

where C is a parameter depending on modulation type. The exact value of C is tabulated in Table III.

TABLE III
C IN AWGN CHANNEL

C	Modulation Type
$\frac{1}{2}$	BPSK
$\frac{3}{4}$	QPSK
$\frac{M-1}{M}$	MPSK
$\frac{M-1}{M}$	MPAM
$1-\left(1-\frac{\sqrt{M}-1}{\sqrt{M}}\right)^2$	MQAM

For the flat Rayleigh fading channel, the average probability of symbol error is

$$\overline{P_s} = \int_0^\infty P_s(x) p_{r_s}(x)\,dx,$$

where $P_s(x)$ is the probability of symbol error in AWGN with SNR = x,

$$p_{r_s}(x) = \frac{1}{\overline{r}_s} e^{-\frac{x}{\overline{r}_s}}$$

and $\overline{r}_s$ is the average SNR per symbol. From [4], the average probability of symbol error is almost the same as (12) except for P_e. The modified P_e is given in Table IV shown in the last page, where $g_{PSK} = \sin^2\left(\frac{\pi}{M}\right)$. Notice that coherence here means the receiver has perfect channel state information (CSI), e.g., the amplitude attenuation, phase influence, and delay time are known at receiver.

Extending our analysis to other fading channels is straightforward. For example, if the channel is a Nakagami-*m* channel, the symbol error rates for M-PAM signal can be obtained by substituting $P_s(x)$ with

$$P_s(x) = \left(\frac{M}{M-1}\right)\left[1-\mu\sum_{k=0}^{m-1}\binom{2k}{k}\left(\frac{1-\mu^2}{4}\right)^k\right]$$

for *m* is integer and $\mu = (3x/[m(M^2-1)+3x])^{1/2}$. On the other hand, if *m* is not an integer, then

$$P_s(x) = \left(\frac{M}{M-1}\right)\frac{1}{\sqrt{\pi}}\frac{\sqrt{3x/m(M^2-1)}}{[(m(M^2-1)+3x)/m(M^2-1)]^{m+1/2}}$$
$$\frac{\Gamma(m+\frac{1}{2})}{\Gamma(m+1)}\ {}_2F_1\left(1, m+\frac{1}{2}; m+1; \frac{m(M^2-1)}{m(M^2-1)+3x}\right)$$

where $\Gamma(\cdot)$ is gamma function and ${}_2F_1$(a,b;c;d) is the Gauss hypergeometric function.

VI. Conclusion

CR has attracted much interest because of its potential to greatly enhance the spectrum utilization efficiency. TDCS is a novel new candidate SS technique that invokes the CR concept. In this report, we consider the effect of spectra mismatches due to spectral estimation error. BER expressions for BPSK signals in various operating conditions are given. We also derive analytical SER expressions for other modulations like MPSK, QAM signals and flat Rayleigh fading channels. Our analysis can easily be extended to other flat-fading channels by deriving the corresponding $P_s(x)$. It is shown that the spectral estimation error results in error floor. As expected, the BER/SER performance is improved and the error floor is reduced when the per-tone (single-subcarrier) detection error decrease. Increasing the number of subcarriers (processing gain) in the SS band also has similar effect. Based on this, it suggests that the best access police is to choice all subbands in terms of BER/SER if the subbands are estimated as idle state. We also find that the BER/SER performance is more sensitive to the spectral estimation error at the receiver than that at the transmitter.

There are quite a few issues that remain to be solved. Firstly, we use a simple Bernoulli distribution to model the estimation error, which is appropriate if the spectral estimation is carried out in a tone-by-tone manner. A more realistic model depends on the spectral estimation method used. It would be interesting to see how the system behaves under different spectral mismatch models. Secondly, a soft decorrelation process might be useful to reduce the impact of spectral mismatches and enhance system performance. Furthermore, cooperative spectrum sensing and prediction should be considered in the future to reduce the mismatch probability.

[References]

[1]. V. Chakravarthy, A. S. Nunez, J.P. Stephens, A.K. Shaw, M.A.Temple, "TDCS, OFDM, and MC-CDMA: A Brief Tutorial,'" *IEEE Commun. Mag.*, vol 43, issue 9, pp. 11 – 16, Sep. 2005.

[2]. V. Chakravarthy, A. K. Shaw, M. A. Temple, J.P. Stephens, "Cognitive radio - an adaptive waveform with spectral sharing capability," in *Proc. IEEE WCNC'05*, vol 2, pp. 724 – 729, 13-17 Mar. 2005

[3]. M. J. Lee *et al.*, ``Wavelet domain communication system: bit error sensitivity characterization for geographically separated transceivers," in *Proc. MILCOM 2002*, Anaheim, CA, vol. 2, pp. 1378–82, Oct. 2002.

[4]. M. K. Simon, M. Alouini, "A unified approach to the performance analysis of digital communication over generalized fading channels,'" in *Proc. IEEE*, vol. 86, issue 9, pp. 1860 – 1877, Sep. 1998.

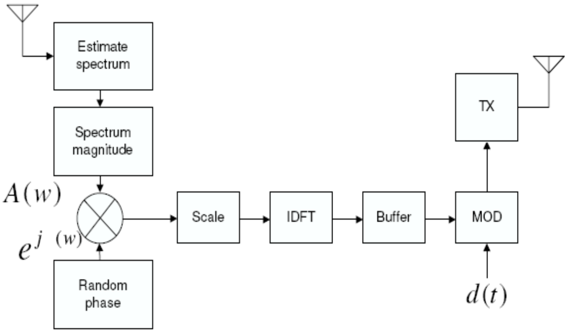

Fig. 1. Block diagram for a TDCS transmitter

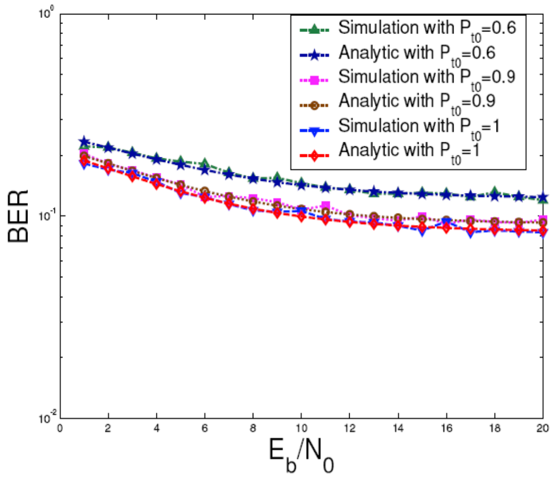

Fig. 2. BER performance for different P_{t0}

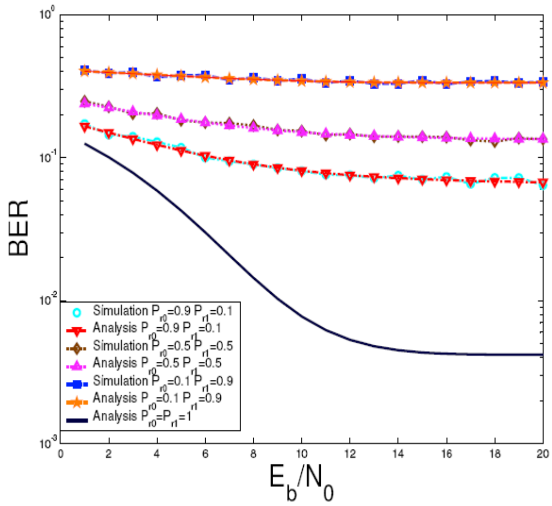

Fig. 3. BER performance for different P_{r0} and P_{r1}

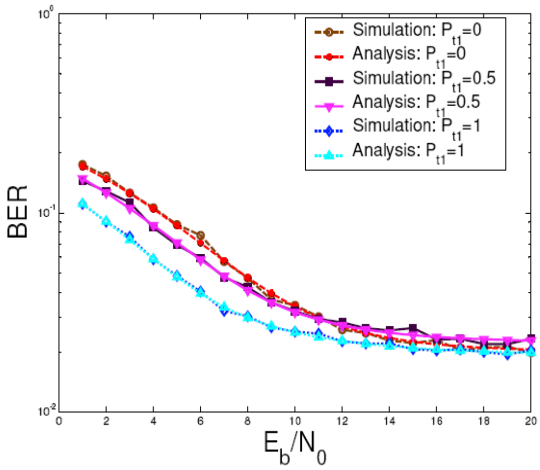

Fig. 4. BER performance for different P_{t1}'s

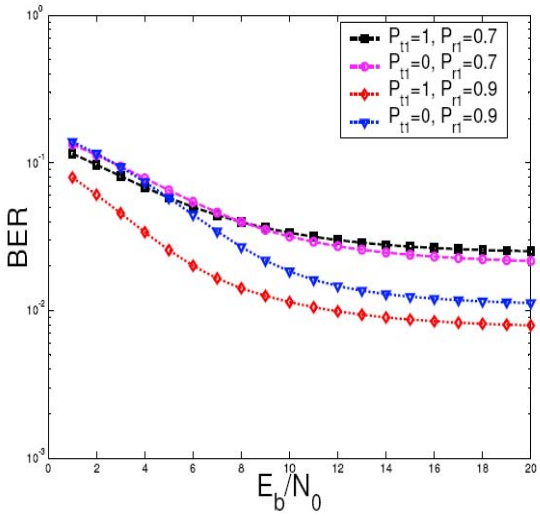

Fig. 5. The effect of interference

TABLE I

EIGHT POSSIBLE SCENARIOS FOR A TDCS LINK.

Case	$(A(\omega), A(\omega)_{\mathrm{Tx}}, A(\omega)_{\mathrm{Rc}})$	The effect of non-ideal match
0	$(0,0,0)$	None
1	$(0,0,1)$	additional noise and interference are introduced in the subband ω
2	$(0,1,0)$	introduce interference to an existing user and reduce the received signal energy
3	$(0,1,1)$	introduce interference to an existing user and interference from existing user to the receiver
4	$(1,0,0)$	None
5	$(1,0,1)$	additional noise in the subband ω is introduced
6	$(1,1,0)$	received signal energy is reduced
7	$(1,1,1)$	None

$$P_b = \sum_{N_1=0}^{N}\sum_{i=0}^{N_1}\sum_{j=0}^{N-N_1}\sum_{k_1=0}^{i}\sum_{l_1=0}^{j}\sum_{k_2=0}^{N_1-i}\sum_{l_2=0}^{N-N_1-j}\binom{N}{N_1}\left(\frac{1}{2}\right)^N\binom{N_1}{i}P_{t0}^{i}(1-P_{t0})^{N1-i}$$
$$\binom{N-N_1}{j}P_{t1}^{N-N_1-j}(1-P_{t1})^{j}\binom{i}{k_1}P_{r0}^{k_1}(1-P_{r0})^{i-k_1}\binom{N_1-i}{k_2}P_{r0}^{k_2}(1-P_{r0})^{N_1-i-k_2}\binom{j}{l_1}P_{r1}^{j-l_1}(1-P_{r1})^{l_1}$$
$$\binom{N-N_1-j}{l_2}P_{r1}^{N-N_1-j-l_2}(1-P_{r1})^{l_2}Q\left(\sqrt{\frac{2E_b(\frac{k_1+l_1}{\max(i+j,1)})}{N_0\left(1+\frac{k_2+l_2}{\max(k_1+l_1,1)}\right)+\frac{l_1+l_2}{\max(k_1+l_1,1)}N_I}}\right) \quad (2)$$

$$P_s = \sum_{N_1=0}^{N}\sum_{i=0}^{N_1}\sum_{j=0}^{N-N_1}\sum_{k_1=0}^{i}\sum_{l_1=0}^{j}\sum_{k_2=0}^{N_1-i}\sum_{l_2=0}^{N-N_1-j}\binom{N}{N_1}P_{sa}^{N_1}(1-P_{sa})^{N-N_1}\binom{N_1}{i}P_{t0}^{i}(1-P_{t0})^{N1-i}$$
$$\binom{N-N_1}{j}P_{t1}^{N-N_1-j}(1-P_{t1})^{j}\binom{i}{k_1}P_{r0}^{k_1}(1-P_{r0})^{i-k_1}\binom{N_1-i}{k_2}P_{r0}^{k_2}(1-P_{r0})^{N_1-i-k_2}\binom{j}{l_1}P_{r1}^{j-l_1}(1-P_{r1})^{l_1}$$
$$\binom{N-N_1-j}{l_2}P_{r1}^{N-N_1-j-l_2}(1-P_{r1})^{l_2}P_e\left(\frac{E_s(\frac{k_1+l_1}{\max(i+j,1)})}{N_0(1+\frac{k_2+l_2}{\max(k_1+l_1,1)})+\frac{l_1+l_2}{\max(k_1+l_1,1)}N_I}\right) \quad (12)$$

TABLE IV

P_e IN FLAT RAYLEIGH CHANNEL

$P_e(x)$	Modulation Type
$\frac{1}{2}\left(1-\sqrt{\frac{x}{1+x}}\right)$	BPSK
$\left(\frac{M-1}{M}\right)\left\{1-\sqrt{\frac{g_{\mathrm{PSK}}x}{1+g_{\mathrm{PSK}}x}}\frac{M}{(M-1)\pi}\left[\frac{\pi}{2}+\arctan\left(\frac{g_{\mathrm{PSK}}x}{1+g_{\mathrm{PSK}}x}\cot\frac{\pi}{M}\right)\right]\right\}$, where $g_{\mathrm{PSK}}=\sin^2\frac{\pi}{M}$	MPSK
$\frac{(M-1)}{M}\left(1-\sqrt{\frac{3x}{M^2-1+3x}}\right)$	MPAM
$2\left(\frac{\sqrt{M}-1}{\sqrt{M}}\right)\left(1-\sqrt{\frac{1.5x}{M-1+1.5x}}\right)-\left(\frac{\sqrt{M}-1}{\sqrt{M}}\right)^2\left(1-\sqrt{\frac{1.5x}{M-1+1.5x}}\left(\frac{4}{\pi}\arctan\sqrt{\frac{M-1+1.5x}{1.5x}}\right)\right)$	MQAM